Vol 13 No 4, April 2004
1009-1963/2004/13(04)/0434-07

Chinese Physics

© 2004 Chin. Phys. Soc.
and IOP Publishing Ltd

Numerical analysis of fluid flow through a cylinder array using a lattice Boltzmann model*

Dong Ping(董 平)[a)†], Feng Shi-De(冯士德)[a)b)], and Zhao Ying(赵 颖)[b)]

[a)] *Division of Civil Engineering, Faculty of Engineering and Physical Sciences, University of Dundee, DD*1 *4HN, United Kingdom*

[b)] *State Key Laboratory of Numerical Modelling for Atmospheric Sciences and Geophysical Fluid Dynamics, Institute of Atmospheric Physics, Chinese Academy of Sciences, P. O. Box* 9804, *Beijing* 100029, *China*

(Received 24 June 2003; revised manuscript received 9 August 2003)

In this paper we present a detailed computational study of an incompressible Newtonian fluid flow across a periodic array of two-dimensional cylinders which is a simplest non-trivial representation of a porous media. A two-dimensional Lattice Boltzmann Method is used to solve the governing Navier–Stokes equation taking into account of viscous dissipation effects and influence of nonlinear fluid drag. Both the flow fields and the Darcy–Forchheimer drag coefficient as a function of the solid volume fraction are calculated for a wide range of flow Reynolds numbers. The predictions were compared with the results from conventional numerical and empirical models for verification. Apart from confirming that inertial effects can cause a significant deviation from Darcy's law for large velocities the results also show that the characteristics of the vorticity field vary considerably as the Reynolds number increases, which will have major implications to the transport of passive particulate substances within the pores and their removal rate.

Keywords: Darcy-Forchheimer drag, porous media, Reynolds number, lattice Boltzmann method
PACC: 0340, 0340G, 0500, 0540

1. Introduction

Flows in porous media can be studied at either the microscopic or the macroscopic scale. For the former scale the flows within individual pores are determined using standard fluid dynamics equations while for the latter scale a continuum description is usually adopted in which methods based on volume averaging are used to derive the pertinent macroscopic governing equations from the equations pertaining to microscopic scales. The linkage between these two descriptions constitute the well known scaling-up problem. It is usually expressed in terms of the permeability as defined in the Darcy's law or its many variants which relate the pressure gradient inside the medium to the area-averaged flow velocity field and viscosity. Although the permeability can in principle provide quantitative correlations between morphological features of pore geometry and its capacity to transmit liquid, its values depend on many factors such as porosity, typical length scale of pore, grain size distribution, anisotropy and tortuosity of pore connections. Therefore, the permeability determined either analytically or empirically for porous media with complex structures involves considerable uncertainty. As the microscopic boundary conditions cannot always be clearly identified in the volume averaged governing equations the solutions of the volume averaged equations may deviate essentially from the volume average of the exact microscopic solution. Such erroneous results could be particularly significant for heterogeneous media with large internal surface.

Due to the complexity of the internal microstructures the flows within porous media are difficult to predict efficiently using most conventional numerical methods. In recent years the lattice Boltzmann method (LBM) has been recognized as a promising numerical tool to investigate flows in highly complex geometries. For example, Rothmann (1988) [1] applied the lattice gas automata to the simulation of porous flows and verified the Darcy's law in simple as well as complicated geometries. Succi *et al* (1989) [2] utilized the LBM to determine the permeability in a 3D random media. The wall effects on hydraulic permeabilities for ordered and disordered media were investigated by Clague *et al* (2000) [3] using the LBM.

*Project supported by the UK Engineering and Physical Sciences Research Council (EPSRC) through a research grant (Grant No GR/R72532/01) and by the Chinese Science Foundation through a grant (Grant No ZKCX2-SW-210, 8-1502).

†E-mail: P.dong@dundee.ac.uk

Their simulation results were in excellent agreement with that of the semi-analytic solutions. In the context of engineering applications of the LBM, Spaid and Phelan (1997) [4] have modified the LBM to solve the Stokes/Brinkman formulation for flow in heterogeneous porous media as occurs in liquid composite moulding processes. The fluid–rock interactions that incorporate the heterogeneity of geological systems and geochemical reactions between fluids and the media through which they flow were studied by O'Brien *et al* (2000).[5]

However, despite the large amount of computational literature on the LB modelling, there seems still a lack of detailed comparisons between the results from the LB models and that from conventional models for complex flows. Such comparisons are crucial, not only for validating LB methods, but also to identify areas of computational difficulties for different types of flow. From the micro-scale results, the permeability tensor can be determined without approximation. In the case of flows passing an array of cylinders, the first such computational experiment was presented by Coulaud *et al* (1988).[6] In that work, a porous medium was represented by cylinders of either equal or unequal diameters arranged in a regular pattern on a square or triangular base. The unsteady Navier–Stokes equations were solved for the microscopic flow in the porous spaces. A more detailed computation was recently performed by Lee and Yang (1997) [7] which also included a detailed comparison of the drag force predicted by both models.[7] Despite the fact that the qualitative behaviour of the flow was reproduced by both models, large quantitative discrepancies exist between the two predictions and an independent calculation will help to explain the reasons for these discrepancies.

In this study, we carried out a detailed computation of a unidirectional steady fluid flow across a periodic array of two-dimensional cylinders forced under a constant pressure gradient. A two-dimensional lattice Boltzmann model for incompressible fluid flow was used. We numerically determined physical properties of the flow field. In addition, the ratio between pressure difference and fluid flux has been calculated exactly to determine the fluid drag coefficient on the basis of Darcy–Forchheimer's law.

2. The lattice Boltzmann model

The existing lattice Boltzmann models can be classified as either the single speed model or the multi-speed model according to the lattice connectivity, i.e. the dependence of the particle velocity on the nearest neighbours, next-nearest neighbours and next-next-nearest neighbours. In the D2Q9 model each lattice point is connected with its four nearest and four next-nearest (diagonal) neighbours while in the D3Q19 model each lattice point is connected to its six nearest (at a distance) and 12 next-nearest neighbours. The more links could potentially lead to more accurate results but at the expense of increasing computational time.

In this work, the computations were carried out using a standard D2Q9 model. It had been extensively tested for simple fluid flows such as Couette flow, Poiseuille flow and the cavity flow where either the analytical solution or numerical solutions using conventional numerical methods are available. Excellent agreements were obtained for each of these cases. Therefore, it is expected that this model is sufficiently accurate for more complex structures such as flows through periodic array of cylinders.

2.1. The model

Simplified BGK equation is adopted for the governing equation of a particle velocity distribution function

$$f_i(r_\alpha + c_{i\alpha}\delta t, t + \delta t) = f_i(r_\alpha, t) - \Omega_i \qquad (1)$$

with

$$\Omega_i = \frac{1}{\tau}\left[f_i(r_\alpha, t) - f_i^{(0)}(r_\alpha, t)\right],$$

where f_i are the particle velocity distribution functions, i is the number of directions of moving particles, α is coordinate index, Ω_i is the collision operator, and τ is the dimensionless relaxation time coefficient; the particle velocity $c_{i\alpha}$ has the same modulus in all moving directions $|c_{i\alpha}| = c = \text{const}$, $c_0 = 0.0$, where c also represents the length of discrete lattice; δt is the discrete time step, r_α is the particle space position, and $f_i^{(0)}$ is the equilibrium velocity distribution function of local particles. In this study we adopted the equilibrium velocity distribution function $f_{ki}^{(0)}$ of Maxwell local particles with the third-order accuracy,

$$f_i^{(0)} = W_i\rho\Big[1 - 2Ec_{i\alpha}u_\alpha + 2E^2(c_{i\alpha}u_\alpha)^2 + Eu^2 - 2E^2c_{i\alpha}u_\alpha u^2 - \frac{4}{3}E^3(c_{i\alpha}u_\alpha)^3\Big], \qquad (2)$$

where ρ and u_α are dimensionless fluid density and velocity, respectively. W_i and E are coefficients determined by relevant conservation law, and can be found

based on the conservation criterion between the mass, momentum, energy and momentum flux of microscopic particles and macroscopic fluids, $\rho = \sum_i f_i^{(0)}$, $\rho u_\alpha = \sum_i f_i^{(0)} c_{i\alpha}$, $\rho u^2 + 2\rho e = \sum_i f_i^0 c^2$. The expressions for W_i and E for several different discrete lattices can be found in Feng *et al* (2001).[8,9] The fluid dynamics equation for an incompressible fluid can be derived by the Chapman–Enskog and Taylor expansion method,

$$\frac{\partial \rho}{\partial t} + \frac{\partial \rho u_\alpha}{\partial r_\alpha} = 0, \tag{3}$$

$$\rho \frac{\partial u_\alpha}{\partial t} + \rho u_\beta \frac{\partial u_\alpha}{\partial r_\beta} = -\frac{\partial P}{\partial r_\alpha} + \nu \frac{\partial^2 u_\alpha}{\partial r_\beta^2}, \tag{4}$$

$$P = \frac{2}{D}\rho\, e; \quad \nu = \frac{2e\delta t}{D}\left(\tau - \frac{1}{2}\right),$$

where e is the internal energy of fluid per unit mass and is a constant ($e = Dc^2/6$), ν is the kinematic viscosity, P is the pressure, and D is the number of spatial dimensions.

2.2. Boundary conditions

The LBM equations given above are subject to specific initial conditions and boundary conditions. The initial conditions at $t = 0$ are $u_x = 0$, $u_y = 0$ and $\rho = 1.0$ everywhere within the flow field $0 \le X \le X_{\max}$, $0 \le Y \le Y_{\max}$. The boundary conditions include the prescribed inflow velocity, U_0, on left boundary which are

$$u_x(0, Y, t) = U_0, \quad u_y(0, Y, t) = 0.0, \tag{5}$$

and a periodic boundary on the left and the right boundaries which are given in terms of the particle velocity distribution as

$$\begin{aligned} f_i(0, Y, t) &= f_i(X_{\max}, Y, t), \\ f_j(X_{\max}, Y, t) &= f_j(0, Y, t); \end{aligned} \tag{6}$$

$$\begin{aligned} u_x(X_{\max}, Y, t) &= u_x(0, Y, t) = U_0, \\ u_y(X_{\max}, Y, t) &= u_y(0, Y, t) = 0.0, \end{aligned} \tag{7}$$

where $f_i(0, Y, t)$ and $f_j(X_{\max}, Y, t)$ are unknown particle velocity distribution functions on the left and right boundaries, respectively. The top and bottom boundaries are: for the velocity field,

$$\frac{\mathrm{d}u_x}{\mathrm{d}y} = \frac{\mathrm{d}u_y}{\mathrm{d}y} = 0 \tag{8}$$

for the particle velocity distribution functions,

$$\frac{\mathrm{d}f_i(X, 0, t)}{\mathrm{d}y} = \frac{\mathrm{d}f_j(X, Y_{\max}, t)}{\mathrm{d}y} = 0. \tag{9}$$

The no-slip condition is implemented on the surface of the cylinders.

In order to facilitate the comparison with previous calculations, the dimensionless variables are defined in a manner similar to that in Lee and Yang (1997) as

$$\begin{aligned} u_x &= \frac{U_x}{U_c}, \quad u_y = \frac{U_y}{U_c}, \\ p &= \frac{P}{\Delta P}, \quad \mathrm{Re} = \frac{U_c L}{\nu}, \end{aligned} \tag{10}$$

where U_x and U_y are the velocity components in the x and y directions,[7] P is the fluid pressure, ΔP is the prescribed pressure gradient in the x direction between the upstream and downstream ends of the flow domain, ν is the kinematic viscosity of the fluid, and $U_c = \sqrt{\Delta P/\rho}$ is the characteristic velocity.

3. Computational results

The flow field consists of a simple horizontal channel with impermeable boundaries and regularly spaced cylinders in its interior. The cylinder row spacing $L = 1$ is taken as the characteristic length scale, and

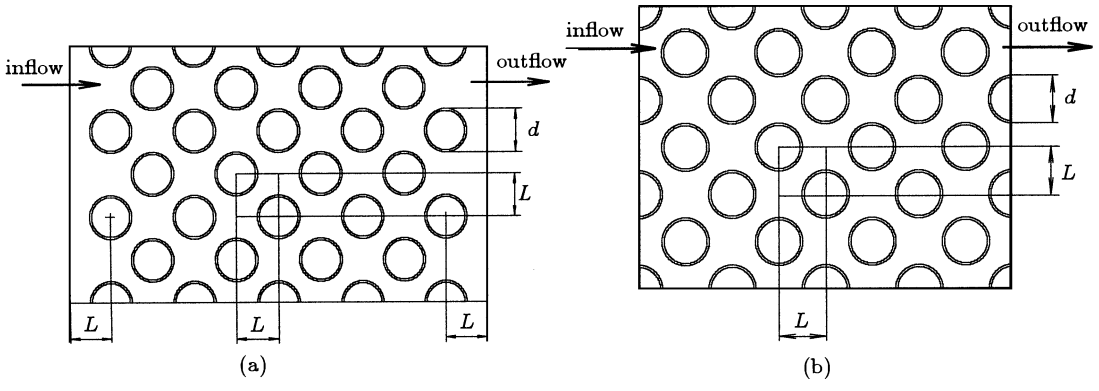


Fig.1. Computational domains with cylinder array configuration, (a) with extra length and (b) without the extra length.

discrete lattice scale is $\delta r = L/N$ where N is the discrete lattice number with N being 75 used here. For any prescribed porosity the diameter of the cylinder d can be determined in term of L. In order to determine the boundary effects computations were carried out for two flow fields with the sizes of $10L \times 6L$ and $8L \times 6L$, respectively and shown as (a) and (b) in Fig.1. The two systems are identical except for the extended sections for (a). The computations were performed for a wide range of Reynolds numbers and porosity. The results presented below are related to the main flow properties.

3.1. Flow fields

It is expected that flow along a channel partially obstructed by cylinder arrays of low porosity (small volume fractions) is sensitive to the porosity as well as the flow or particle Reynolds number. This can be seen in Fig.2 which shows the simulated results of the main fluid properties for flows at three Reynolds numbers. From Figs.2(a) and (c), it is seen that the streamlines and isobars are symmetric about the vertical line through the centre of the cylinder for both Re=1.0 and Re=10.0. This linear behaviour is to be expected as the viscous friction dissipation is dominant over the fluid drag under low Reynolds number. With Re being increased to 30 however, the streamlines and isobars become asymmetric indicating the increasing importance of the drag force. The asymmetry in isobars is most pronounced indicating the presence of considerable pressure drag. This transition in flow states can be best seen in Fig.2(b) which shows the distribution of vorticity. From Re=1 to Re=10, the strength of the vorticity increases by one order of magnitude but the distribution remains symmetric while for Re=30, the increase in vorticity strength is accompanied by a large distortion in symmetry of its distribution. Considerable vorticity is swept to the lee side of the cylinder, which could have major implications to the transport of passive particulate substances within the pores and particularly their removal rate. Comparison has been made with the calculations by Lee and Yang (1997) and good qualitative agreements have been achieved in all cases.[7] Detailed comparisons and further discussions will be presented in the next section in connection with the drag forces.

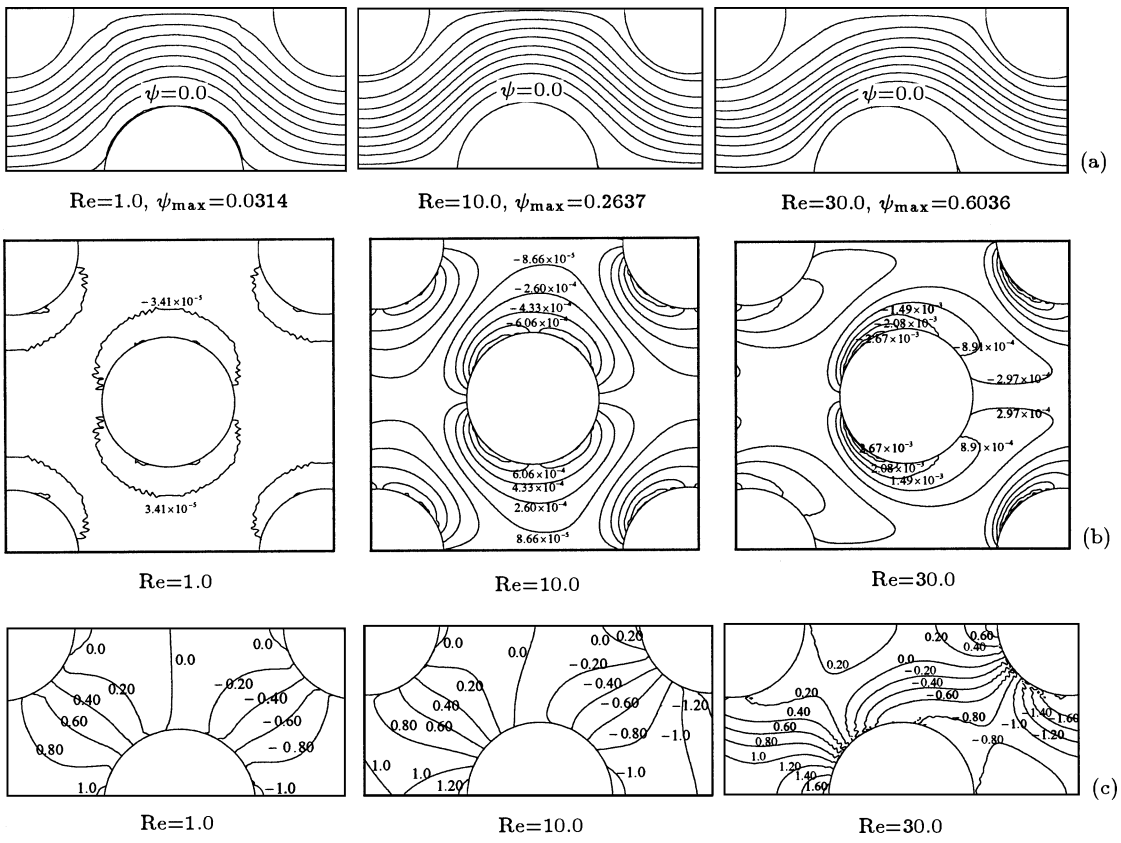


Fig.2. Calculated (a) streamlines, (b) vorticities and (c) pressure contours for the flow field with d/L=0.8, Re=1.0 (Re_d=0.02396), Re=10.0 (Re_d=2.2497) and Re=30.0 (Re_d=15.334).

3.2. The Darcy–Forchheimer drag

In engineering applications, it is not practical to perform calculations at the pore scale. Instead, empirical formulae for the bulk resistance are widely used. As originally proposed by Darcy (1856) [10] and later extended by Forchheimer (1901) [11] and Ergun (1952) [12] the pressure force can be expressed (for one-dimensional flow) as

$$-\frac{\mathrm{d}\bar{P}}{\mathrm{d}X} = \frac{\Delta P}{L} = \frac{\mu}{K}\bar{U} + \frac{C_E}{K^{1/2}}\rho|\bar{U}|\bar{U}, \qquad (4)$$

where μ being the viscosity of the fluid and K the permeability of the porous solid matrix. This expression can be written in an alternative form as

$$-\frac{\mathrm{d}\bar{P}}{\mathrm{d}X} = \frac{\Delta P}{L} = \left(\frac{d^2}{K} + F\mathrm{Re}_d\right)\frac{\mu\bar{U}}{d^2}. \qquad (5)$$

The term in the brackets to be denoted as DF is the Darcy–Forchheimer (DF) drag with F being the Forchheimer coefficient. For flow regimes at higher velocities, Ergun (1952) constructed a correlation which relates the Darcy–Forchheimer drag to the fluid parameters (velocity, viscosity, and density) and the porous media matrix parameters (porosity, permeability, surface condition of particles),[12] which reads

$$\frac{d^2}{K} + F\mathrm{Re}_d = \alpha\frac{(1-\varepsilon)^2}{\varepsilon} + \beta\frac{1-\varepsilon}{\varepsilon^3}\mathrm{Re}_d. \qquad (6)$$

The porosity ε for a unit cell is given by

$$\varepsilon = 1 - \left(\frac{\pi}{8}\right)\left(\frac{d}{L}\right)^2. \qquad (7)$$

Figure 3 shows the computed DF drag vs the granule Reynolds number Re_d at various porosities for the two computation domains. Both results agree with each other in the overall trends and in the details over a large part of the parameter range. Slight discrepancies are noticeable at the smaller porosity or high Re_d. This is believed to be due to the inaccuracies of the boundary conditions at the edges of computational domain (b).

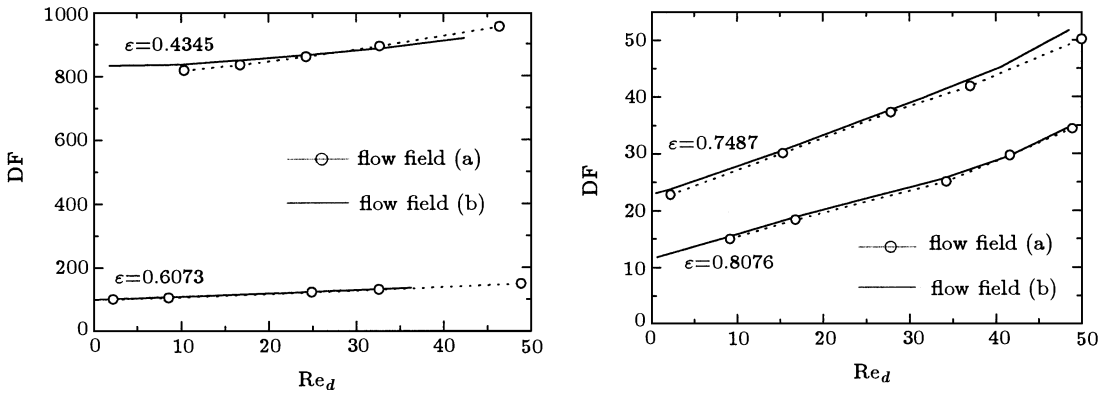


Fig.3. Comparison of the Darcy–Forchheimer drag between the flow fields (a) and (b) for the LBM.

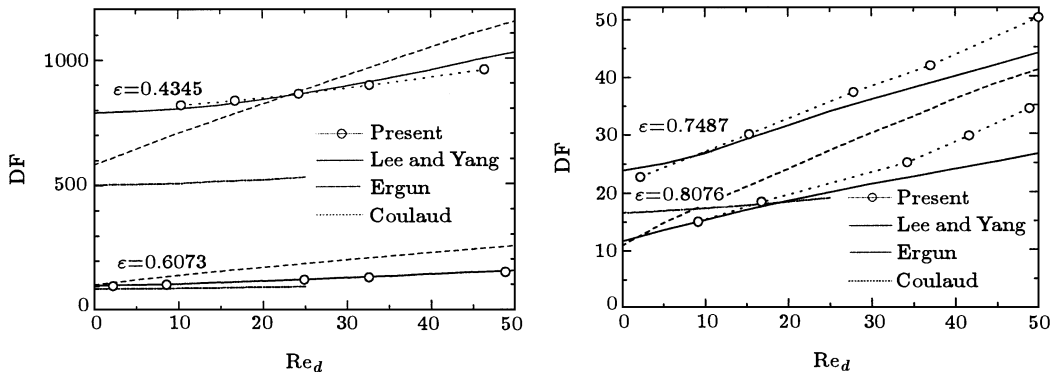


Fig.4. Comparison of the Darcy–Forchheimer drag between the present LBM result and for ε=0.4345, 0.6073, 0.7487, 0.8076.

Figure 4 shows a comparison with the results from Lee and Yang (only the results from computational domain (a) are given here). The calculations based on Ergun (1952) and by Coulaud *et al* (1987) are also shown in the same figure for completeness. A linear vertical scale rather than a log scale is used here to show the difference more clearly. As can be observed, the agreement with the results by Lee and Yang is good when the porosity is low but significant discrepancies are present when the porosity is large. The LBM predictions are systematically greater than that of Lee and Yang (1997) when Re_d are greater than 10 and the discrepancy also increases with Re_d. It is noted, that for large porosity, the LBM predictions are between that of Ergun and Lee and Yang. Considering that Ergun's correlation is based on experiments of flow through beds of granular solids with the predictions by Coulaud *et al* generally lying well below these curves, this result can be viewed as an independent verification of the qualitative fidelity of the numerical models. Lee and Yang has discussed the possible reasons for the underestimation by Coulaud *et al* which include the smoothing effects due to the conjugated gradient algorithm employed and the coarse grid system. It is suspected that the weighted function scheme employed by Lee and Yang, although accurate for the linear terms, could also have some averaging effects on the nonlinear terms of the governing N-S equations and thus underestimates the nonlinear drag.

It should be pointed out that the nonlinearity existing in the real porous media flows could be attributed to a number of sources. Fluid turbulence, microscopic inertial forces and increased microscopic drag forces are the three most commonly suggested causes. However, the experimental evidence indicates that nonlinear dependence appears well before the onset of real turbulence (Scheidegger, 1974).[13] Neither the present model nor other models for microscopic calculations have included the effects of turbulence although the empirical model by Ergun may implicitly account for such effects in the data especially at high Reynolds numbers. In addition, it should be recognized that the macroscopic inertial forces are not the cause of the first change of flow, even if they can be approximated by a quadratic term (Ruth and Ma, 1992 [14]). Using both the hybrid mixture theory (Hassanizadeh and Gray, 1987 [15]) and averaging (Ruth and Ma, 1992), it has been shown that the important nonlinear term arises from terms involving integrals over the solid–liquid interface as the result of increased microscopic drag forces or microscopic inertial forces which indirectly distort the area integral term by affecting the pressure and velocity fields. Both effects are fully accounted for by the present and other microscopic models.

4. Conclusions

In this paper we have taken a microscopic approach to study fluid flows through an ideal porous media represented by an array of cylinders using a lattice Boltzmann model. The numerical experiments reveal that the spatial distribution of flow field properties such as streamlines, isobars and vorticities are symmetrical for small Reynolds number but become asymmetric when Re is great. The degree of asymmetry increases with the Reynolds number. It is also shown that the Darcy–Forchheimer drag can be well predicted by both the present and Lee & Yang's models but discrepancies between the two models grow with the porosity and Reynolds number. Under such conditions, the present predictions lie between the results from Ergun's empirical formula (1952) and that of Lee & Yang.[7,12] Although more computations may be required to further check the accuracy of all the numerical models to date, it is believed that the model predictions presented here is sufficiently reliable due to the intrinsic simplicity of the LB model used and the low grid sensitivity.

References

[1] Rothmann D H 1988 *Geophysics* **53** 509

[2] Succi S, Foti E and Higuera F 1989 *Europhys. Lett.* **10** 433

[3] Clague D S, Kandhai B D, Zhang R and Sloot P M A 2000 *Phys. Rev.* E **61** 616

[4] Spaid M A A and Phelan F R 1997 *Phys. Fluids* **9** 2468

[5] O'Brien G, Bean C J and McDermott P F 2000 *J. Geochem. Explor.* **69** 119

[6] Coulaud O, Morel P and Caltagirone J P 1988 *J. Fluid Mech.* **190** 393

[7] Lee S L and Yang J H 1997 *Int. J. Heat Mass Transfer* **40** 3149

[8] Feng S D and Tsutahara M 2001 *Chin. Phys.* **10** 587
[9] Feng S D, Mao J Y and Zhang Q 2001 *Chin. Phys.* **10** 1103
[10] Darcy H 1856 *Les Fontaines Publiques de la Ville de Dijon*, Ed. Victor Dalmont, Paris, France
[11] Forchheimer P 1901 *Z. Ver. Deutsch. Ing.* **45** 1782
[12] Ergun S 1952 *Chem. Eng. Progr.* **48** 199
[13] Scheidegger A E 1974 *The Physics of Flow through Porous Media* (Toronto: University of Toronto Press)
[14] Ruth D W and Ma H 1996 *Transport in Porous Media* **7** 255
[15] Hassanizadeh S M and Gray W G 1987 *Transport in Porous Media* **2** 521